X International Conference on Computational Methods in Marine Engineering
MARINE 2023
J. García-Espinosa, L. González, J.E. Gutiérrez & B. Serván-Camas (Eds)

The Fixed Grid Fully Non-linear Potential Flow Model REEF3D::PTF - Examination of Different Methods for Solving The Laplace Equation at the Free Surface

Fabian Knoblauch[1*], Ahmet Soydan[2], Widar Wang[3] and Hans Bihs[4]

[1,2,3,4] Department of Civil and Environmental Engineering, Norwegian University of Science and Technology, Høyskoleringen 7a, 7491 Trondheim, Norway

[*] Corresponding author: Fabian Knoblauch, fabian.knoblauch@ntnu.no

ABSTRACT

The evaluation of forces acting on marine structures and modelling the complex fluid-body interaction of floating structures is crucial in marine engineering. While current CFD models based on the Navier-Stokes equation are able to represent the behaviour of floating bodies with great accuracy, fully non-linear potential flow solvers are able to model realistic extreme sea states at a fraction of usual computational costs. A Finite Difference based fully non-linear potential flow model with the ability to represent complex fluid-structure interaction and floating, would therefore be a major advantage for the design of marine structures. The first step is hereby the solver itself.
Therefore the fully non-linear potential flow model REEF3D::PTF is developed, using a Finite Differences Scheme. A level set function is used for free surface representation and an immersed boundary method is used to enforce boundary conditions. The free surface potential and location are advanced in time, while the potential field is gained from solving the Laplace Equation. Different numerical methods for solving the Laplace Equation at the free surface are developed, implemented and tested. Comparison, to analytical values, experimental data and the σ-grid solver REEF3D::FNPF show a high sensibility of the fixed grid solver REEF3D::PTF regarding the used free surface treatment method in the Laplace Equation. Since this sensibility is found to be the main reason for small remaining inaccuracies, the fixed grid model PTF shows to have great potential to be further perfected and suitable for future implementation of complex structures and floating bodies. Thus, the future work will focus on addressing this sensitivity and optimise the free surface treatment for improved accuracy and reliability.

Keywords: Computational Fluid Dynamics; ; Potential Flow; Non-linear; REEF3D; Finite Differences Method; Marine Engineering.

NOMENCLATURE

g	Gravitation constant
h	Water depth at stillwater level
i	Numerical index for Finite Difference Scheme
t	time
$\vec{v}$	Velocity vector
x	First horizontal coordinate
y	Second horizontal coordinate
z	Vertical coordinate
η	Vertical free surface position
∇	Nabla operator
ϕ	Velocity potential
$\bar{\bar{\cdot}}$	Tensor
$\vec{\cdot}$	Vector

1. INTRODUCTION

The evaluation of wave loads acting on marine structures and floating objects is crucial for their design. Non-linear waves in extreme sea states result in especially high structural loads and should therefore be considered in the safety evaluation and design process. Current developments in the field of Computational Fluid Dynamics allow to model complex fluid structure interaction, including floating structures and force calculation (Martin et al., 2021). At the current state, the CFD solvers, able to represent floating structures in complex, highly non-linear waves are mainly built upon solving the Navier-Stokes equation, like in Martin et al. (2021). For numerical modelling of non-linear ocean waves and extreme sea states, fully non-linear potential flow solvers have proven to be a suitable tool (Bihs et al., 2020), as compared to common Navier-Stokes solvers, fully non-linear potential flow solvers allow for accurate wave representation at a fraction of the usual computational costs (Bihs et al., 2020). Regarding the method used to model fully non-linear potential flow, different approaches exist. Newest Spectral Element models, as the one by Ducrozet et al. (2012), as well as Boundary Element models, as presented in Grilli (1996) and Grilli et al. (2001), allow for modelling of non-linear waves. However SEM models fail to fully represent strong refraction and reflection (Wang et al., 2022) , while BEM models suffer from their mathematical complexity regarding full asymmetrical matrices (Wang et al., 2022). A Finite Differences Method approach has first been presented by Li & Fleming (1997) and and followed up in a detailed accuracy analysis by Bingham & Zhang (2007) Recent examples for advanced fully non-linear potential solvers are given by Wang et al. (2023) and Engsig-Karup et al. (2012). Like other non-linear potential flow solvers, these use a σ-coordinate grid, for increased computational stability (Xu, 2021) (Bihs et al., 2020) (Engsig-Karup et al., 2012). This impedes the implementation of floating structures (Xu, 2021), as the sigma grid coordinate transformation compels the availability of a water height value for the entire domain. Therefore a fully nonlinear potential flow model using a fixed coordinate grid is needed, to allow for future implementation of a floating algorithm by the means of an FDM solver. For boundary condition implementation most current approaches, like Xu et al. (2021), use an Immersed Boundary method which has first been described by Peskin (1972). Regarding boundary conditions and Immersed Boundary implementation, the major difference between a fixed grid potential flow solver and a σ-grid solver is, that the domain does not follow the free surface. This causes the stencil, used for discretising the Laplace equation, to reach across the free surface and out of the fluid. Thus a free surface treatment method to the Laplace equation needs to be derived for a fixed grid fully non-linear potential flow FDM solver. In Xu et al.

(2021) an approach is derived, by solving an interpolation scheme at the free surface, using Ghost Cells outside of the fluid region. Further ambitions of Xu (2021) and Xu et al. (2023), to implement bodies into the solver presented in Xu et al. (2021), have not reached the stage of floating. Furthermore, no detailed tests of the free surface treatment method implemented in Xu et al. (2021) and Xu (2021) have been presented.
In this study, approaches different to the one presented by Xu et al. (2023) shall be examined. Therefore a fixed grid fully non-linear potential flow solver is built and different free surface treatment methods are implemented for solving the Laplace Equation. The solvers stability and precision is evaluated in different test cases. The results of different free surface treatment methods are compared to the results of a potential flow solver using a σ-coordinate grid and to experimental data. The overall goal is to maximise the stability and precision of the fully non-linear potential flow solver, by adapting the optimal free surface treatment method. This shall allow for further implementation of floating structures in the developed solver. A fully non-linear potential flow solvers highly reduced computational costs make it preferable over a CFD simulation, when several different designs and layouts shall be tested. A fully nonlinear potential flow solver, able to implement floating structures, would therefore allow a tighter integration of the numerical analysis into the design process, which benefits the iterative progress and creates clarity regarding the design's safety and efficiency.

2. NUMERICAL MODEL

2.1 Governing Equations

Under the assumption of an irrational flow, the velocity field can be defined as the gradient of a velocity potential ϕ.

$$\vec{v} = \nabla\phi \tag{1}$$

The assumption of irrationality prevents the consideration of viscosity and turbulence, as turbulence itself is a rotational phenomenon. The governing equation for incompressible potential flow is a Laplace equation which follows from the incompressible continuity equation.

$$\nabla \cdot \vec{v} = 0 \tag{2}$$

$$\nabla^2\phi = 0 \tag{3}$$

The Laplace equation of the velocity potential is solved in the domain by the application of suitable boundary conditions. The boundary condition for the sea bed follows from the prohibition of flow through the sea bed.

$$\frac{\partial\phi}{\partial z} + \frac{\partial h}{\partial x}\frac{\partial\phi}{\partial x} + \frac{\partial h}{\partial y}\frac{\partial\phi}{\partial y} = 0\Bigg|_{z=-h} \tag{4}$$

Whereas $h = h(x)$ denotes the water depth from the sea bed to the stillwater level. On the free surface η, a kinematic boundary condition can be derived from the relation of the velocity at the free surface to the velocity of the free surface itself.

$$\frac{\partial\eta}{\partial t} = -\frac{\partial\eta}{\partial x}\frac{\partial\phi}{\partial x} + \frac{\partial\eta}{\partial y}\frac{\partial\phi}{\partial y} + \frac{\partial\phi}{\partial z}\left(1 + \frac{\partial^2\eta}{\partial x^2} + \frac{\partial^2\eta}{\partial y^2}\right)\Bigg|_{z=\eta} \tag{5}$$

Further, a dynamic boundary condition for the free surface can be derived by usage of Bernoulli's Equation and the assumption of a constant atmospheric pressure along the free surface.

$$\frac{\partial\phi}{\partial t} = -\frac{1}{2}\left(\frac{\partial^2\phi}{\partial x^2} + \frac{\partial^2\phi}{\partial y^2} - \left(\frac{\partial\phi}{\partial z}\right)^2\left(1 + \frac{\partial^2\eta}{\partial x^2} + \frac{\partial^2\eta}{\partial y^2}\right)\right) - g\eta\Bigg|_{z=\eta} \tag{6}$$

2.2 Numerical Implementation

The Boundary Value Problem described in section 2.1 is solved numerically by usage of a Finite Differences Scheme on a structured, staggered grid (Li & Fleming, 1997). The boundary conditions are implemented via an Immersed Boundary method, using Ghost Cells to implicitly enforce the boundary conditions in the domain (Peskin, 1972).
At the inlet, a wave generation zone of minimum one wavelength is used in combination with a relaxation function (Mayer et al., 1998) (Jacobsen et al., 2012). At the outlet, a numerical beach of minimum two wavelengths is used to dissipate waves and avoid reflections. The numerical beach is based on a relaxation method as well.
The free surface is defined by a level set method using a signed distance function (Sussman et al., 1994).
The Laplace equation is discretised by the second-order central difference scheme. Wave propagation in time is defined by the free surface boundary conditions. The convective terms of these are discretised by the fifth-order weighted essentially non-oscillatory (WENO) scheme (Jiang & Shu, 1996).
The discretised Laplace equation is solved with the parallelised geometric multi-grid algorithm given by hypre (van der Vorst, 1992). Parallelisation is achieved by domain decomposition and solving for each domain fracture on a different CPU. Communication across the domain fractures is realised via Ghost Cells, which are updated from the adjacent CPUs using MPI.
For advancing in time, a third-order TVD Runge-Kutta scheme is used (Shu & Osher, 1988). The time step size is determined adaptively to keep a constant CFL number defined by the phase velocity.

2.3 Solving the Laplace Equation at the Free Surface

The temporal part of the numerical model is given by the free surface boundary conditions in equation 5 & 6. The correct evaluation of spatial derivatives at the free surface is hence crucial for the precision and stability of the simulation. This sets high demands for the stencils used at the free surface. Since there are no values for the velocity potential above the free surface, the vertical derivative $\partial\phi/\partial z$ uses an upwind stencil built upon ϕ at the free surface, and the six elements below. The horizontal derivatives for the free surface boundary conditions are taken along the free surface, using a fifth-order WENO scheme.
At the free surface, the central difference scheme used for discretising the Laplace equation 3 reaches out of the fluid domain. Therefore the ordinary Central difference scheme needs to be adapted at the free surface, and a definition for the values of ϕ at the free urface interception point needs to be clarified. Since the simulation is sensitive regarding values at the free surface, the choice of stencil modification and ϕ definition are expected to have a significant impact on the solvers stability and precision.
Four different methods of defining the relation at the free surface are implemented and tested for their impact on the solver's stability and precision. The test results are presented in section 3. All implemented methods have in common, that they determine the value of ϕ for each spatial dimension independently, and also independent of the definitions used for other cells. To explain this in more detail, first the ordinary central difference scheme for solving the Laplace equation in one spatial dimension is presented.

$$\frac{\phi_{i-1} - 2\phi_i + \phi_{i+1}}{\Delta x_{i-1,i}\ \Delta x_{i,i+1}} = 0 \tag{7}$$

This stencil is applied in each spatial direction, leading to a linear equation system which is solved by hypre.

$$\overline{\overline{M}}\vec{\phi} = \vec{0} \tag{8}$$

The matrix is solved for the entire domain, whereas the stencil is only built for points below the free surface, therefore the centred values ϕ_i are always available. For points above the free surface, all values are set zero. At the free surface a non-centre value of the stencil might be situated outside of the free surface. In that case one of the four following options can be used to substitute for that value.

The first method uses the value determined for the free surface below the point. Since the free surface values originate from the DFSBC in equation 6, they are known and not solved for in equation 8.
The second method uses the absolute values of the signed distance function for the adjacent points below and above the free surface as spatial distances to interpolate linear between the free surface value above the centred point and the free surface value below the point above the free surface. Additionally, the terms of the stencil around the free surface are weighted by the ratio of the two absolute signed distance function values.
The third method is in many parts identical to the second method. The difference between them is, that the third method does not weight the stencil terms by the signed distance function ratio. Instead the signed distance function values are used to determine the relative position of the free surface between the two points around it. The relative position of the free surface is used to modify the Δx of that part of the stencil accordingly.
The fourth method uses a three node Laplace Interpolation scheme at the free surface, with the signed distance function values as spatial distances, to determine the interpolated free surface value to be used and to weight the stencil terms.

3. STABILITY AND ACCURACY ANALYSIS

Two different test setups are used to investigate the solver's stability and precision. The first one is a numerical wave tank used to simulate the propagation of 2nd-order Stokes waves. This case is chosen since Stokes waves are non-linear, but offer the option of comparing to a theoretical mathematical solution.
The second test case are waves propagating over a submerged bar. This case offers the possibility to observe effects implied by the sea bed contour, such as shoaling. Furthermore experimental data is available for the second test case (Beji & Battjes, 1993).
In all tests it became clear, the fourth implemented method for free surface treatment of the Laplace Equation, using a three node Laplace Interpolation, is generally unstable in its current implementation, as it tends to crash in most cases due to an ill-defined matrix. Therefore no values can be presented for the fourth method.

3.1 Stokes 2nd-order Wave Tank

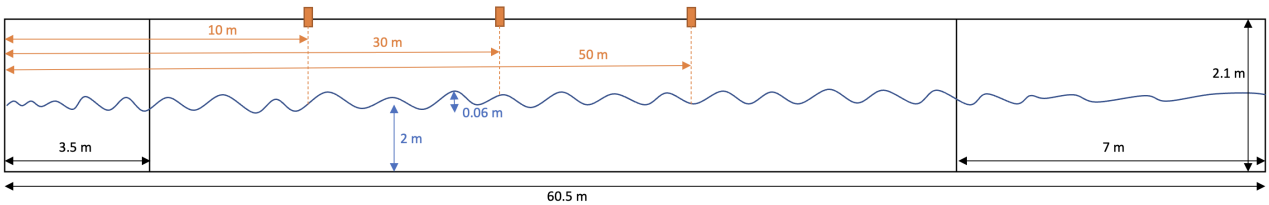

Figure 1: Two-dimensional numerical wave tank used to inspect 2nd-order Stokes-wave propagation.

The solver is tested for wave propagation in a 2D numerical wave tank as shown in figure 1. Regular 2nd-order Stokes-waves with a wave height of $H = 0.06\ m$ and a wave period of $T = 1.43\ s$ are created

in a wave generation zone of 3.5 m, using a relaxation function. The overall length of the tank is chosen as 60.5 m and the stillwater level is 2 m. The last 7 m of the tank are defined as a numerical beach, where waves are dissipated by a relaxation function to avoid reflection. Wave gauges are are placed at a distance of 10 m, 30 m and 50 m to the beginning of the wave tank. Since a mathematical formulation of 2nd-order Stokes-Waves exists, the data from the numerical wave gauges can be compared to an analytical solution. The idea behind this setup is to investigate numerical dispersion and diffusion as the waves propagate. Since these properties depend on mesh resolution, two different mesh sizes are used. The coarser one using $N_x = 160$ nodes in x-direction and $N_z = 15$ nodes in z-direction, while the fine mesh consists of $N_x = 1600$ horizontal and $N_z = 50$ vertical nodes. Both meshes are refined in vertical direction around the stillwater level at 2 m using a sinus hyperbolicus with a factor of 4.5. The setup is tested with all four methods presented in section 2.3 as well as with REEF::3D FNPF, a fully non-linear potential flow solver using a σ-grid coordinate transformation (Bihs et al., 2020).

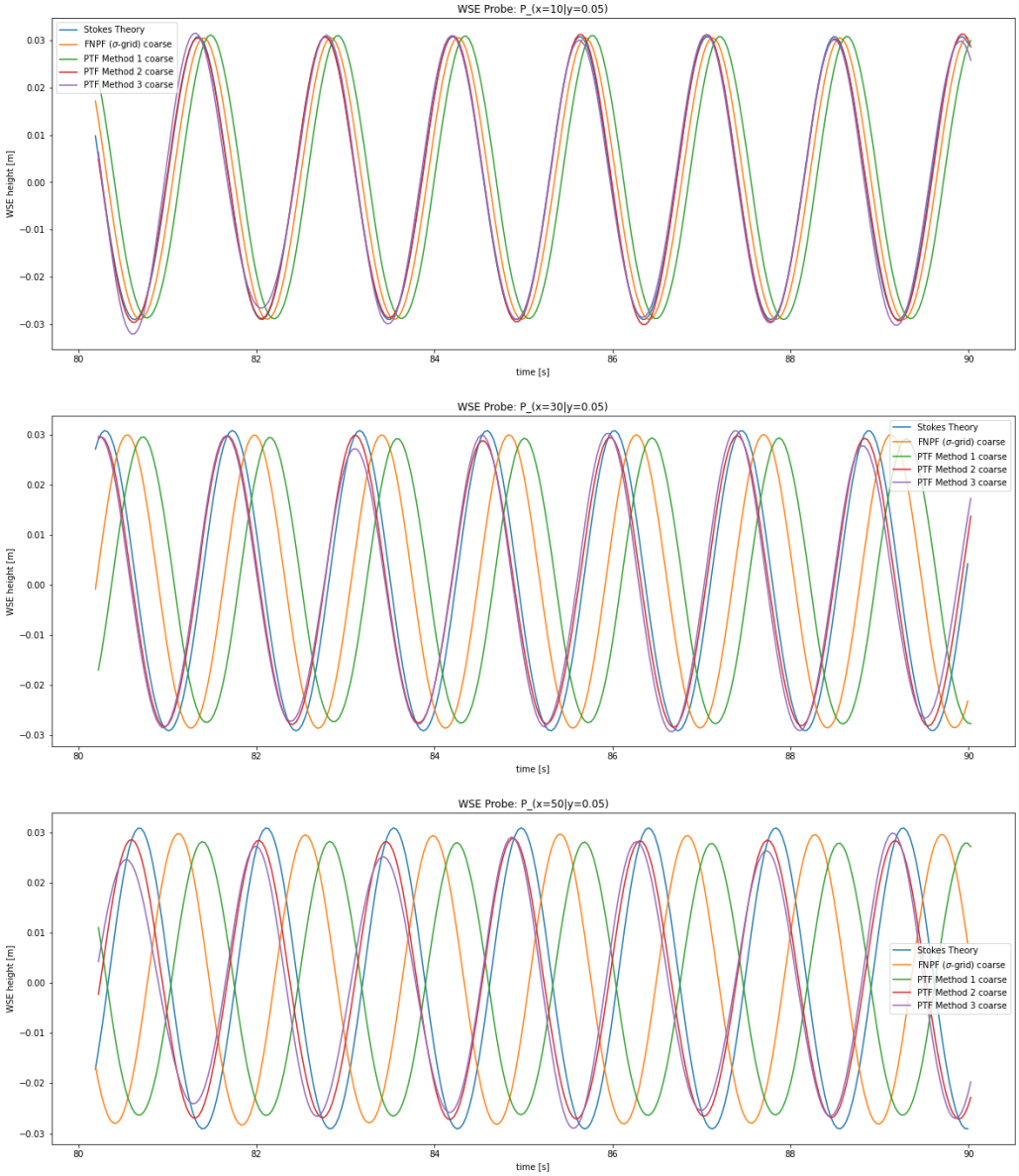

Figure 2: Wave gauge data for the coarse Stokes 2nd-order Wave tank setup ($N_x = 160, N_z = 15$).

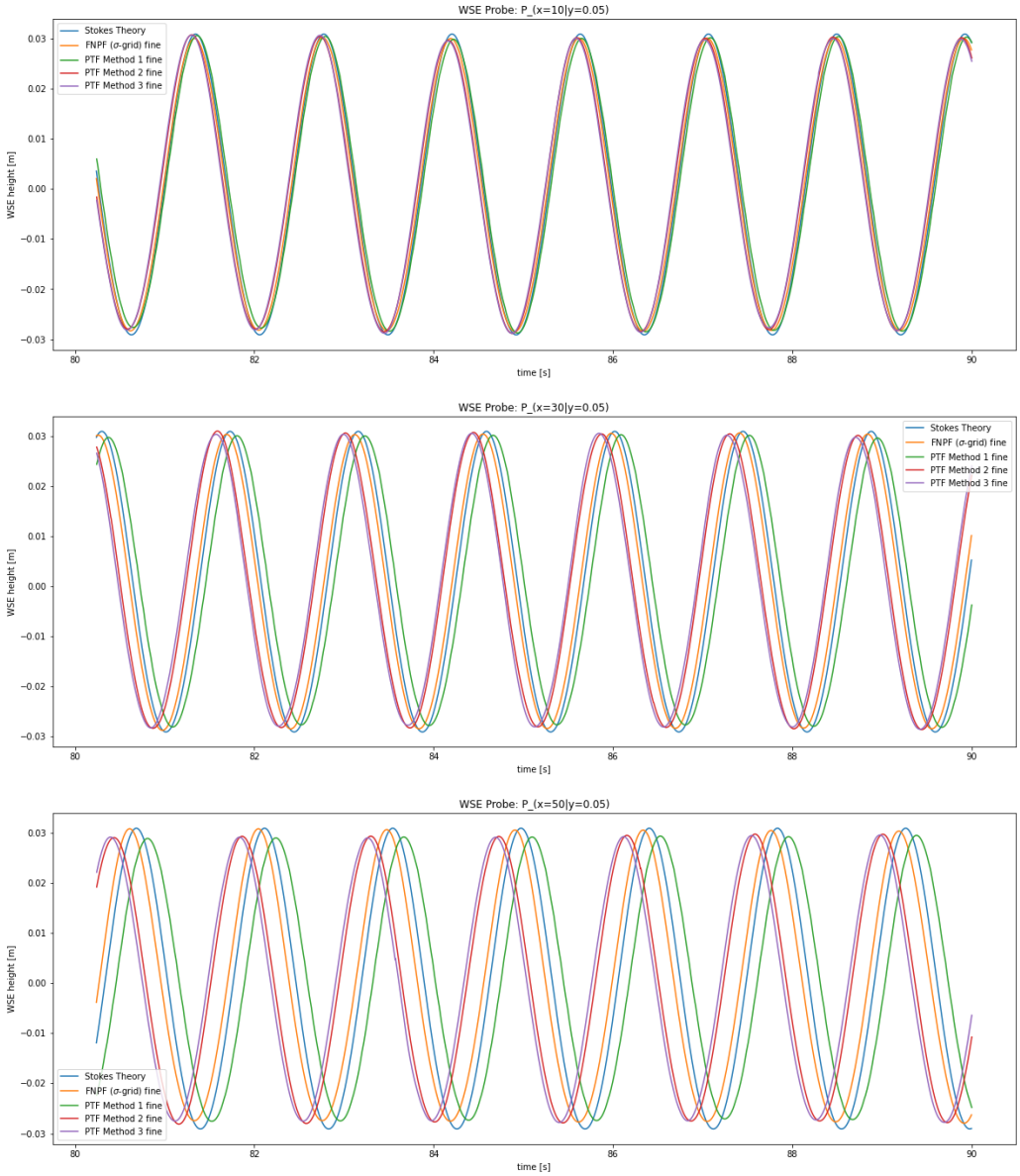

Figure 3: Wave gauge data for the fine Stokes 2nd-order Wave tank setup ($N_x = 1600, N_z = 50$).

Figure 2 and figure 3 both show, that numerical diffusion is generally slightly larger for the PTF solver, than for FNPF using a σ-grid. Further, the numeric diffusion of Method 3 seems to be irregular for a coarse resolution, but levels in with the other methods for the fine resolution. Regarding dispersion, Method 1 shows a large backwards phase shift for the coarse resolution, which gets smaller for the finer resolution. Contrary to that, Method 2 and 3 feature a small forwards phase shift for the coarse resolution, which increases with the finer mesh. The FNPF solver has a small backwards phase shift for the coarse grid and a small forwards phase shift for the fine grid. It must be noted, that the setup has been tuned to benefit the needs of PTF, for example regarding the vertical mesh refinement factor. The settings are thus suboptimal for FNPF.

3.2 Submerged Bar Test Case

The second test case of a submerged bar originates from an experimental study presented in Beji & Battjes (1993), therefore experimental data for comparison is available. The numerical implementation is again two-dimensional. Specifications for the test case are shown in figure 4. The mesh resolution is set as $N_x = 2000$ horizontal nodes and $N_z = 60$ vertical nodes, with a vertical refinement around the stillwater level at $0,4\ m$ using a sinus hyperbolicus with a factor of 4.5. Wave gauges are located at $x = 4.0\ m,\ 10.5\ m,\ 12.5\ m,\ 13.5\ m,\ 14.5\ m,\ 15.7\ m,\ 17.3\ m,\ 19.0\ m$ (Bihs et al., 2020).

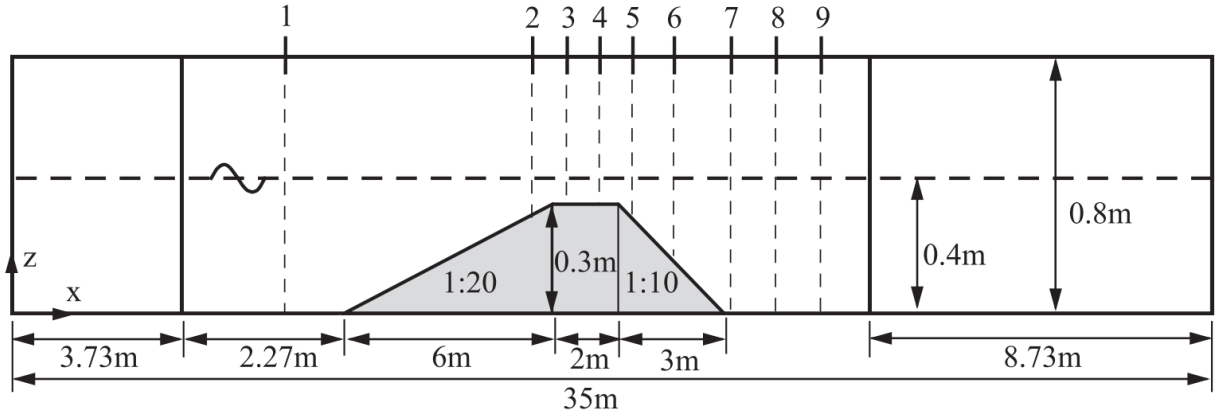

Figure 4: Two-dimensional submerged bar test case (Bihs et al., 2020)

Regular waves with a wave height of $H = 0.01\ m$ and a wavelength of $L = 3.75\ m$ are generated in the $3.73\ m$ long wave generation zone at the beginning of the tank. The last $8.73\ m$ are defined as a numerical beach. The setup is tested with all four methods presented in section 2.3 as well as REEF::3D FNPF, a fully non-linear potential flow solver using a σ-grid coordinate transformation (Bihs et al., 2020).

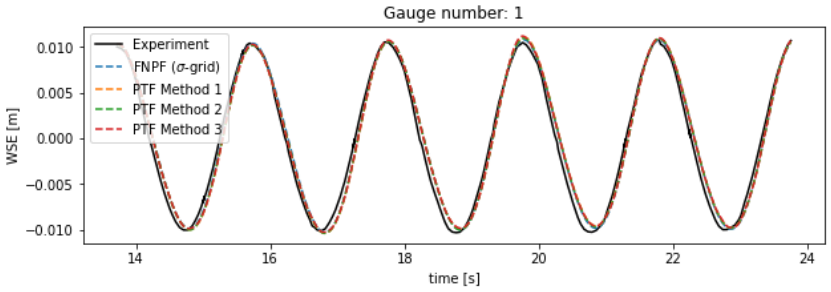

Figure 5: Water surface elevation of submerged bar test at probe 1

For the submerged bar test case, good conformity can be found for the upwards shoaling of the incoming waves (figure 5) up to the end of the submerged plateau (figure 6). Up from the bar's decreasing part at Probe 5 (figure 7 differences between the models and the experimental data increase gradually with the downward shoaling. Especially Method 2 and Method 3 overshoot at the higher wave peaks and have a slight forward phase shift, while Method 1 seems to overshoot the secondary peaks at probe 9 (figure 10). Overall FNPF shows the best ability, while again it has to be mentioned, that the setup has been tuned to benefit the needs of PTF. The settings are thus suboptimal for FNPF.

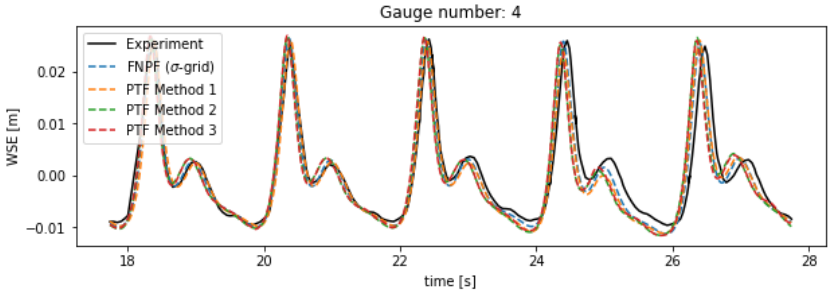

Figure 6: Water surface elevation of submerged bar test at probe 4

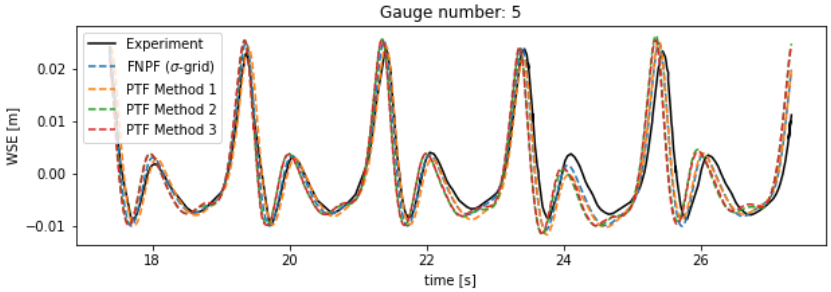

Figure 7: Water surface elevation of submerged bar test at probe 5

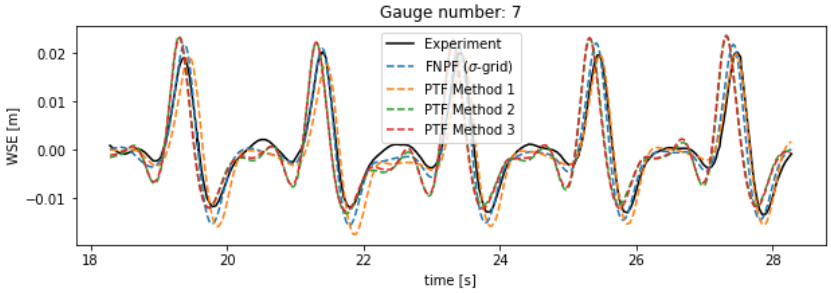

Figure 8: Water surface elevation of submerged bar test at probe 7

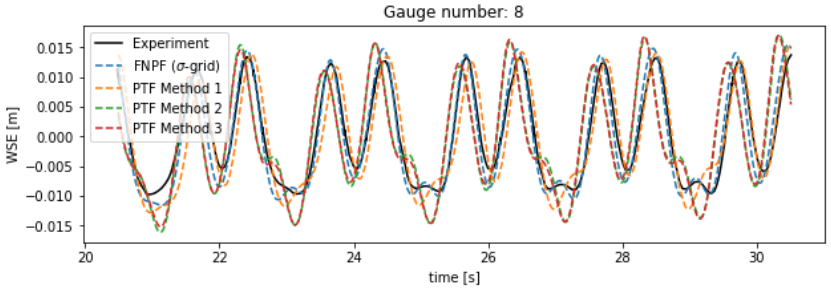

Figure 9: Water surface elevation of submerged bar test at probe 8

4. CONCLUSION

A fully non-linear potential flow solver has been developed, which uses a domain with a fixed Cartesian coordinate system, instead of a σ-grid, and therefore allows the future implementation of overhanging

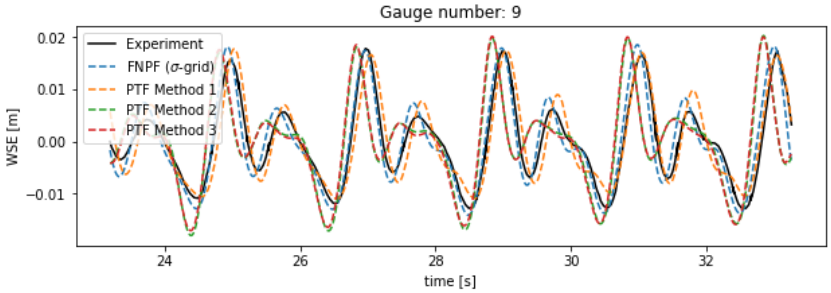

Figure 10: Water surface elevation of submerged bar test at probe 9

or floating structures. Due to the domain not following the free surface, special methods for free surface handling in the equation system used for solving the Laplace Equation have been proposed, implemented and tested. Two test cases have been examined The first one investigated the numerical diffusion and dispersion for 2nd-order Stokes Waves. It was found that the choice of free surface treatment method is significant for the phase shift, observable at coarse resolution. The second test case, propagation over a submerged bar (Beji & Battjes, 1993), showed, that all models can accurately capture the upward shoaling effect, but inaccuracies manifest during the downward shoaling, also depending on the used free surface treatment method.
Overall it can be concluded, that the current implementation of the fixed grid fully non-linear potential flow solver PTF is still less stable and precise, than the σ-grid solver FNPF. Nonetheless PTF shows the ability to simulate non-linear waves and wave-bottom interaction with a small error. Furthermore this error proves to be mainly dependent on the treatment of the free surface intersection in the solving scheme of the Laplace Equation. Since only a few methods have been implemented and tested, there is a significant potential that PTF can reach the same stability and precision as FNPF with an improved method for free surface treatment in the Laplace Equation. Thus, the future work will focus on addressing this sensitivity and optimise the free surface treatment for improved accuracy and reliability.

5. ACKNOWLEDGEMENTS

The authors are grateful for the grants provided by the Research Council of Norway under the IPIRIS project (no. 308843). Some simulations were performed on resources provided by Sigma2 - the National Infrastructure for High Performance Computing and Data Storage in Norway.

REFERENCES

Beji, S., & Battjes, J. (1993). Experimental investigation of wave propagation over a bar. *Coastal Engineering*, *19*(1), 151–162.
URL `https://www.sciencedirect.com/science/article/pii/037838399390022Z`

Bihs, H., Wang, W. W., Pâkozdi, C., & Kamath, A. (2020). Reef3d::fnpf - a flexible fully nonlinear potential flow solver. *Journal of Offshore Mechanics and Arctic Engineering*, *142*, 1–12.

Bingham, H., & Zhang, H. (2007). On the accuracy of finite-difference solutions for nonlinear water waves. *Journal of Engineering Mathematics*, *58*, 211–228.

Ducrozet, G., Bonnefoy, F., Le Touzé, D., & Ferrant, P. (2012). A modified high-order spectral method for wavemaker modeling in a numerical wave tank. *European Journal of Mechanics - B/Fluids*, *34*, 19–34.

Engsig-Karup, A., Madsen, M., & Glimberg, S. (2012). A massively parallel gpu-accelerated model for analysis of fully nonlinear free surface waves. *International Journal for Numerical Methods in Fluids*.

Grilli, S. (1996). Fully nonlinear potential flow models used for long wave runup prediction. *Long-Wave Runup Models*.

Grilli, S., Guyenne, P., & Dias, F. (2001). A fully nonlinear model for three-dimensional overturning waves over arbitrary bottom. *International Journal for Numerical Methods in Fluids*, *35*, 829–867.

Jacobsen, N., Fuhrman, D., & Fredsoe, J. (2012). A wave generation toolbox for the open-source cfd library: Openfoam (r). *International Journal for Numerical Methods in Fluids*, *70*.

Jiang, G.-S., & Shu, C.-W. (1996). Efficient implementation of weighted eno schemes. *Journal of Computational Physics*, *126*(1), 202–228.
URL https://www.sciencedirect.com/science/article/pii/S0021999196901308

Li, B., & Fleming, C. A. (1997). A three dimensional multigrid model for fully nonlinear water waves. *Coastal Engineering*, *30*(3), 235–258.
URL https://www.sciencedirect.com/science/article/pii/S0378383996000464

Martin, T., Tsarau, A., & Bihs, H. (2021). A numerical framework for modelling the dynamics of open ocean aquaculture structures in viscous fluids. *Applied Ocean Research*, *106*, 102410.
URL https://www.sciencedirect.com/science/article/pii/S014111872030969X

Mayer, S., Garapon, A., & Sørensen, L. S. (1998). A fractional step method for unsteady free-surface flow with applications to non-linear wave dynamics. *International Journal for Numerical Methods in Fluids*, *28*(2), 293–315.

Peskin, C. S. (1972). Flow patterns around heart valves: A numerical method. *Journal of Computational Physics*, *10*(2), 252–271.
URL https://www.sciencedirect.com/science/article/pii/0021999172900654

Shu, C.-W., & Osher, S. (1988). Efficient implementation of essentially non-oscillatory shock-capturing schemes. *Journal of Computational Physics*, *77*(2), 439–471.
URL https://www.sciencedirect.com/science/article/pii/0021999188901775

Sussman, M., Smereka, P., & Osher, S. (1994). A level set approach for computing solutions to incompressible two-phase flow. *Journal of Computational Physics*, *114*(1), 146–159.
URL https://www.sciencedirect.com/science/article/pii/S0021999184711557

van der Vorst, H. A. (1992). Bi-cgstab: A fast and smoothly converging variant of bi-cg for the solution of nonsymmetric linear systems. *Society for Industrial and Applied Mathematics.SIAM Journal on Scientific and Statistical Computing*, *13*(2), 631–14. Copyright - Copyright] © 1992 Society for Industrial and Applied Mathematics; Zuletzt aktualisiert - 2022-10-20.
URL https://www.proquest.com/scholarly-journals/bi-cgstab-fast-smoothly-converging-variant-c

Wang, W. W., Pâkozdi, C., Kamath, A., & Bihs, H. (2023). Fully nonlinear phase-resolved wave modelling in the norwegian fjords for floating bridges along the e39 coastal highway. *Journal of Ocean Engineering and Marine Energy*, (pp. 1–20).

Wang, W. W., Pâkozdi, C., Kamath, A., Fouques, S., & Bihs, H. (2022). A flexible fully nonlinear potential flow model for wave propagation over the complex topography of the norwegian coast. *Applied Ocean Research*, *122*, 103103.

Xu, Y. (2021). *A figh-order finite difference method with immersed-boundary treatment for fully nonlinear wave-structure interaction*. Ph.D. thesis, Technical University of Denmark. DCAMM Special Report No.S302.

Xu, Y., Bingham, H. B., & Shao, Y. (2021). Finite difference solutions for nonlinear water waves using an immersed boundary method. *International Journal for Numerical Methods in Fluids*, *93*(4), 1143–1162.
URL `https://onlinelibrary.wiley.com/doi/abs/10.1002/fld.4922`

Xu, Y., Bingham, H. B., & Shao, Y. (2023). A high-order finite difference method with immersed-boundary treatment for fully-nonlinear wave–structure interaction. *Applied Ocean Research*, *134*, 103535.
URL `https://www.sciencedirect.com/science/article/pii/S0141118723000767`